

A peer-reviewed version of this preprint was published in PeerJ on 30 April 2018.

[View the peer-reviewed version](https://doi.org/10.7717/peerj.4656) (peerj.com/articles/4656), which is the preferred citable publication unless you specifically need to cite this preprint.

Silva MdA, Leite YKdC, Carvalho CESd, Feitosa MLT, Alves MMdM, Carvalho FAdA, Neto BCV, Miglino MA, Jozala AF, Carvalho MAMd. 2018. Behavior and biocompatibility of rabbit bone marrow mesenchymal stem cells with bacterial cellulose membrane. PeerJ 6:e4656 <https://doi.org/10.7717/peerj.4656>

Behavior and biocompatibility of rabbits bone marrow mesenchymal stem cells with bacterial cellulosic membrane

Marcello Silva Alencar ¹, Yulla Klinger Carvalho ¹, Camila Ernanda Carvalho ², Matheus Tajra Feitosa ², Fernando Aécio de Amorim Carvalho ³, Bartolomeu Cruz Viana ⁴, Maria Angélica Miglino ⁵, Ângela Faustino Jozala ⁶, Maria Acelina Carvalho ^{Corresp. 1, 2}

¹ Biotechnology Graduate Program / Integrated Center of Morphology and Stem Cell Research (NUPCelt/UFPI), Federal University of Piauí, Teresina, Piauí, Brazil

² Animal Science Graduate Program, Integrated Nucleus of Morphology and Stem Cell Research, Federal University of Piauí, Teresina, Piauí, Brazil

³ Antileishmania Activities Laboratory, Federal University of Piauí, Teresina, Piauí, Brazil

⁴ Department of Physics, Advanced Microscopy Multiuser Laboratory, Laboratory of Physics Material, Federal University of Piauí, Teresina, Piauí, Brazil

⁵ Department of Surgery, Faculty of Veterinary Medicine and Animal Science, University of São Paulo, São Paulo, São Paulo, Brazil

⁶ Laboratory of Toxicological Research, University of Sorocaba, Sorocaba, São Paulo, Brazil

Corresponding Author: Maria Acelina Carvalho
Email address: mcelina@ufpi.edu.br

Introduction: Tissue engineering is being redesigned through promising studies that present great potential to create biomaterials capable of forming functional tissues. The cellular expansion and integration depends very much on the quality and adequacy of the surface of the scaffold being determinant for the success in the biological implants. The objective of this research was to characterize and evaluate *in vitro* the behavior of rabbits Bone Marrow Mesenchymal Stem Cells (BMMSC) when associated with Bacterial Cellulose Membrane (BCM) verifying the adhesion, expansion, cells integration into the biomaterial and the capacity macrophage activation as well as the evaluation of the bacterial cellulosic membrane cytotoxicity and toxicity. **Materials and methods:** Samples of rabbit bone marrow and mesenchymal stem cells were collected and mesenchymal stem cells were isolated from the medullary aspirates for fibroblast colony forming unit (CFU-F) assays, osteogenic and chondrogenic cellular differentiation induction, cellular integration study to the bacterial cellulosic membrane by Scanning Electron Microscopy (SEM) in the time interval of 1, 7 and 14 days as well as cytotoxicity (NO induction), BCM toxicity (MTT) and phagocytic activity. **Results:** The CFC-F assay showed cells with fibroblastoid morphology organized in colonies distributed across the culture area surface. In the growth curve two phases (lag and log) were observed in the course of 15 days. The cells multipotentiality was evident after osteogenic and chondrogenic lineages induction. Regarding the BMMSC bioelectrical integration to BCM, in the first 24 hours, the BMMSC were anchored in the BCM. On the seventh day of culture the cytoplasm was scattered and on fourteenth day the cells were fully integrated into the biomaterial. In the phagocytic activity assay there

was a significant macrophages activation and for the nitric oxide concentrations and MTT analysis no cytotoxic biomaterial was observed. **Conclusion:** The bacterial cellulosic membrane allowed the bone marrow progenitor cells expansion and biointegration with stable cytotoxic profile thus presenting itself as biomaterial with potential for tissue engineering.

Behavior and Biocompatibility of rabbits bone marrow Mesenchymal Stem Cells with bacterial cellulosic membrane

Marcello A. Silva¹; Yulla K. Carvalho¹; Camila E. Carvalho²; Matheus L. Feitosa²; Fernando A. Carvalho³, Bartolomeu C.Viana ^{4,5} Maria Angélica Miglino⁶, Ângela F. Jozala⁷; Maria Acelina M. Carvalho^{1,2}

¹ Biotechnology Graduate Program, Integrated Nucleus of Morphology and Stem Cell Research, Federal University of Piauí, Teresina, Piauí, Brazil.

² Animal Science Graduate Program, Federal University of Piauí, Teresina, Piauí, Brazil.

³ Antileishmania Activities Laboratory, Federal University of Piauí, Teresina, Piauí, Brazil.

⁴ Advanced Microscopy Multiuser Laboratory, Federal University of Piauí, Teresina, Piauí, Brazil.

⁵ Department of Physics, Laboratory of Physics Material, Federal University of Piauí, Teresina, Piauí, Brazil.

⁶ Department of surgery. Faculty of Veterinary Medicine and Animal Science - USP, São Paulo, Brazil.

⁷ Laboratory of Toxicological Research, University of Sorocaba - UNISO, Sorocaba, São Paulo, Brazil.

Corresponding Author:

Marcello A. Silva¹

Email address: dr.marcelloalencar@outlook.com

Maria Acelina M. Carvalho^{1,2}

Email address: mcelina@ufpi.edu.br

Introduction: Tissue engineering has been redesigned by promising studies, presenting a great potential to create biomaterials capable to develop functional tissues. The cellular expansion and integration depends the quality and scaffold surface determinant factors for the success biological implants. The objective of this research was characterize and evaluate *in vitro* characteristics of rabbits Bone Marrow Mesenchymal Stem Cells (BMMSC) associated with Bacterial Cellulose Membrane (BCM) the propose was verify the adhesion, expansion, cells integration into the biomaterial and the capacity of macrophage activation as well as the evaluation of the bacterial cellulosic membrane cytotoxicity and toxicity.

Materials and methods: Samples of rabbit bone marrow were collected. Mesenchymal stem cells were isolated from the medullary aspirates in order to obtain fibroblast colony forming unit (CFU-F) assays. Osteogenic and chondrogenic cellular differentiation induction was done. Cellular integration study to the bacterial cellulosic membrane by Scanning Electron Microscopy (SEM) using 1, 7 and 14 days interval also were done as well as cytotoxicity (NO induction), BCM toxicity (MTT) and phagocytic activity.

Results: The CFC-F assay showed cells fibroblastoid morphology organized in colonies and distributed across the culture area surface. In the growth cells curve, were detected two phases (lag and log) were observed on 15 days. The cells multipotentiality was evident after osteogenic and chondrogenic lineages induction. Regarding the BMMSC bioelectrical integration to BCM, on the first 24 hours, the BMMSC were anchored in the BCM. On the seventh day of culture the cytoplasm was scattered and on fourteenth day the cells were fully integrated into the biomaterial. About phagocytic activity assay there was a significant macrophages activation and for the nitric oxide concentrations and MTT analysis no cytotoxic biomaterial was observed.

Conclusion: The bacterial cellulosic membrane allowed the bone marrow progenitor cells expansion and biointegration with stable cytotoxic profile thus presenting itself as biomaterial with potential for tissue engineering.

Subjects: Biotechnology, Cell Biology, Engineering Tissue, Translational Medicine.

Key-words: Stem Cells; Tissue Engineering; Culture Techniques; Biocompatible Materials; Cellulose.

Introduction

Researchers have been studying bone marrow mesenchymal stem cells, the cells applicability in regenerative medicine and improving methodologies presented a greater effectiveness (Dimarino, Caplan & Bonfield, 2013; Wei et al., 2013; Li et al., 2016).

The mesenchymal stem cells use appears promising in the regenerative medicine field. On the other hands, these studies developed, were investigations involving cardiovascular events (Castellanos et al., 2016), immunological dysfunctions (Kaplan, Youd & Lodie, 2011; Zao, Ren & Han, 2016), bone repair (Emmet et al., 2016), cartilaginous and intervertebral disc (Blanquer, Grijpma, Poot, 2015), tendinosis (Peach et al., 2017), hematological malignancies (Wang, Qu & Zhao, 2012), among others (Squillaro, Peluso & Galderisi, 2016; Schnitzler et al., 2016;).

The tissue engineering comprises a promising multidisciplinary field that involves materials development or devices capable of specific interactions with biological tissues (Langer & Vacanti, 2016). The researches expansion in this area has accentuated the search for subsidies to suport the stem cells biocompatibility in biopolymers to attend *in vitro* tissues develops to replace injured areas.

In the last years a wide variety of biomaterials has been developed showing different physico-chemical and mechanical properties for biomedical purpose. These including tissue regeneration, drug delivery systems, new vascular grafts or *in vitro* and *in vivo* tissue engineering supports (Lin, Lien & Yeh, 2013; Yan *et al.*, 2013; Soheilmoghaddam, Sharifzadeh & Pour, 2014; Zulkifli, Hussain & Rasad, 2014; Pires, Bierhalz & Moraes, 2015; Kim & Kim, 2015; Urbina, Algar & García-Astrain, 2016).

The scaffold success (3D framework) in tissue engineering depends in part of the cellular interest in surface contact determining how this material can be biointegrable and/or biodegradable. The scaffold surface can generate cellular responses, affecting the adhesion, proliferation, migration, biointegration and cellular function. This interaction presents an extreme importance in the medical implants effectiveness being able to define their degree of rejection (Abbott & Kaplan, 2016; Achatz *et al.*, 2016).

In tissue engineering the bacterial cellulose supported the researches interest because it is an abundant biopolymer in nature with biodegradability and able to be synthesized by several bacteria adding the low cost in its manufacture. The nanofibrils formed between 20-100nm. Their which intertwine forming a network and allied to its molecular structure, giving its high hydrophilicity. Many biomedical researches have already used the bacterial cell membrane *in vitro*, in preclinical studies such as drug, hormone and protein release system, artificial skin (Fu, Zhang & Yang, 2013), cartilage (Cruz, Severo & Azzolin 2016), meniscos (Achatz, Kuat & Pfeifer, 2016), intervertebral disc (Flávaro, Arruda & Vialle 2016), valvular prosthesis, artificial cornea and urethra (Rajwade, Paknikar, & Kumbhar, 2015). However it's necessary to deepen the Bacterial Cellulosic Membrane (BCM) biointegration and biodegradation knowledge when associated with Bone Marrow Mesenchymal Stem Cells (BMMSC).

This research propose was characterized and evaluated *in vitro* the rabbit BMMSC behavior when associated with BCM checking the adhesion, expansion, cellular integration into

the biomaterial and the activation macrophages capacity besides the BCM cytotoxicity and toxicity.

Material and Methods

Study Design

A one year old male New Zealand rabbit considered clinically healthy, was used for the isolation procedure of BMMSC. A mouse *Mus musculus* was used as a peritoneal macrophages source. For the cellular viability determination trypan blue and subsequent graphical representation in the growth curve were done. For the fibroblastoid colony forming units (CFU-F) assay were used cells collected from the bone marrow cultured in petri dish in the sixth passage. For the differentiation potential in mesenchymal lineages study were used the means of chondrogenic and osteogenic induction. In the verification of BMMSC biointegration to BCM confocal microscopy and Scanning Electron Microscopy (SEM) were used and to analyze the BCM phagocytic capacity, toxicity and cytotoxicity were used peritoneal macrophages. This study was carried out in strict accordance with the recommendations of the Guide for the Care and Use of Laboratory Animals of the National Institutes of Health. The protocol was approved by the Ethics Committee on the Use of Animals of the Federal University of Piauí (Permit Number: 268/16).

Anesthetic protocol for bone marrow collection

After solid anesthetic fasting of 4 hour and 2 hours of liquids, the rabbit was chemically restrained with a combination of 35 mg / kg of Ketamine Hydrochloride and 3 mg / kg of midazolam maleate. Was performed the major trochanter region trichotomy, antisepsis followed by femoral puncture with a 5mL syringe, 40x12mm needle previously heparinized to obtain a Bone Marrow (BM) sample. The aspirate was conducted to unidirectional laminar flow (VECO FUH 12) for BMMSC. For antibacterial prophylaxis, 10 mg / kg of enrofloxacin were given twice a day for 7 days and 25 mg / kg of Sodium Dipyrone plus 3 mg / kg of tramadol were administered twice daily for 3 days for pain control.

BMMSC rabbit isolation, cultivation and expansion

The medullary aspirate of 1.5mL was diluted in PBS (Phosphated Buffered Saline) in a

ratio of 1:1 in 50mL conical tubes. The resulting contents were filtered in 100µm meshes and deposited in a 15mL conical tube containing Ficoll® (Ficoll Histopaque, SIGMA® no. 17544652) in a ratio of 1:1 (1 of Ficoll® to 1 of bone marrow) and centrifuged at 1,500 rpm for 10 minutes at 20 °C aiming at the cellular constituents separation by density gradient.

The whitish halo, rich in mononuclear cells, was aspirated with an automatic pipettor (Houston®) and immediately diluted in sterile PBS with 1% antibiotic (100 U / mL penicillin, 100 µg /mL streptomycin) for cell lavage and re-centrifuged at 1,500 rpm for 10 minutes at 4°C. Bone marrow samples were resuspended in complete (Invitrogen® low glucose, 11995065) Dulbecco's Modified Eagle's (D-MEM) growth medium, containing 3.7 g / L sodium bicarbonate and 10-15 mM HEPES (Invitrogen® N°. 15630080), pH 7.5, 15% fetal bovine serum (Invitrogen Corporation, no. 16000-044), 1% penicillin streptomycin, 1% L-glutamine (Invitrogen® no 25030081) and 1% non-essential amino acids (Sigma® n° M7145) and thus a cell viability assessment was performed. For this purpose a 50µL aliquot of each sample was diluted in 50µL Trypan Blue dye 0.2% (Invitrogen® n° 15250061) and homogenized in a sterilized glass vial for further cell counting in the Neubauer chamber.

The cells were seeded in a six-well cell culture plate (TPP®) at density of 106 cells/well in 2.0mL of DMEM Low Glucose culture medium supplemented, kept in an incubator (Thermo Scientific Series II Water Jacket) at 37°C in 5% CO2 and 95% humidity. The wells were washed twice every 3 days with PBS solution containing 1% antibiotic (100U/ml penicillin, 100µg/ml streptomycin) followed by the cell culture medium complete exchange until cultures reaching 80% confluence. Subsequently, the culture wells were subjected to trypsinization with 2.0mL 1x trypsin (Invitrogen®, n° 25200-114, 10x Trypsin-EDTA solution) and incubated at 37°C for five minutes. After this period the trypsin action was inactivated with addition of 4.0mL of D-MEM Low Glucose medium supplemented. The solution was transferred to a 15mL conical bottom tube and centrifuged (FANEM refrigerated Cytocentrifuge MOD.280R Excelsa 4) at a temperature of 20°C and 1,500rpm for 10 minutes.

The supernatant was completely discarded, the pellet resuspended in 1.0 mL of full D-MEM, and a new cell count was performed. These cells in suspension were used for cell expansion. For this purpose were plated 10⁶ cells / mL in 25 cm² tissue culture bottles with 3.0mL of supplemented DMEM culture medium. These were incubated at 37°C in 5% CO2 and

155 95% humidity. The cultures were expanded and photographed under an inverted phase contrast
156 microscope (COLEMAN NIB-100®) and peaked with twice the original area, and the cell
157 concentration was checked at each passage.

158 **Cell viability assessment**

159 The cell count which determines the samples concentration and viability was performed
160 using the Trypan Blue exclusion method. After addition and homogenization of 30µL of the cell
161 suspension in 30µL of the Trypan Blue solution (50µL of 4.25% sodium chloride in 200µL of
162 Trypan Blue), a 10µL aliquot in Neubauer Chamber was observed under an optical microscope
163 10x objective). The BMMSC growth curve was performed in duplicate by sowing the
164 concentration of 1×10^4 cells/mL in five six-well plates counting two wells every 24 hours in the
165 course of 15 days. The culture medium of the plates was changed every 3 days to maintain
166 nutrient availability.

167 **Fibroblastoid colony-forming unit assay**

168 After plating 1×10^6 cells/mL of the BMMSC rabbit fraction, culture media exchanges
169 were carried out the culture medium exchanges until the well delimited colonies maximum
170 formation in the Petri plate surface 90x15mm. The plate was observed daily for the colonies
171 formation with more than 30 cells. Cells were fixed with 4% paraformaldehyde for 30 minutes
172 and stained with Giemsa for 10 minutes at the local temperature washing the excess with
173 distilled water. The colonies were observed and counted macroscopically on the Petri dish
174 surface.

175 **Cell differentiation**

176 The cell differentiation potential analysis was performed with BMMSC samples in the
177 sixth passage (P6) cryopreserved in liquid nitrogen for 12 months. They were thawed and sown
178 in 25cm² bottles for cell expansion until reaching 80% confluence. After that period the culture
179 was trypsinized and seeded at the concentration according to protocol established by the
180 manufacturer for chondrogenic and osteogenic differentiation.

181 For chondrogenic cell differentiation, 3×10^5 well cells were seeded in the 96-well plate.
182 After 48 hours the spheroid bodies formation was observed and then the culture medium
183 replaced by the Stem Pro Chondrogenesis Differentiation Kit. The medium exchange was

maintained every three days during the 21 day period. The analysis was performed on histological sections with blades stained with Alcian Blue.

In the osteogenic differentiation assay, 6×10^4 cells were seeded in a 24-well plate. Initially, the supplemented culture medium was removed and replaced with the osteogenic induction medium, changed every 3 days during the 21 day period. During this period cells present in the culture morphological characteristics were evaluated. After osteogenic differentiation detection the cell evaluation was performed by Alizarin Red staining that identifies the calcium rich extracellular matrix, characteristic of the osteoblasts presence.

The cell monolayer was washed with PBS and fixed with 10% AP for 30 minutes at room temperature when the AP was removed and the cell monolayer was washed with distilled water and covered with Alizarin Red for 5 min. Subsequently, the dye was removed and five washes were performed with distilled water, the calcium-rich extracellular matrix and the calcium amount deposit were recorded under an inverted light microscope.

Analysis of the BMMSC biointegration to BCM

For the study of BMMSC expansion and biointegration to BCM was used the concentration of 2×10^4 cells in 12 well plates. They were cultured on BCM in three distinct times (1, 7 and 14 days). The BMMSC were fixed to BCM using 3% glutaraldehyde washed once with PBS and further dehydrated by slow water exchange using a series of ethanol dilutions (30%, 55%, 70%, 88%, 96% and absolute) during 20 minutes at each concentration. For analysis by SEM (FEI Quanta FEG 250) the samples were fixed to the stub with double-sided carbon tape and taken to the dehumidifier for 2 hours and then metalized with gold.

Phagocytic activation

The phagocytic activity test was performed by collecting resident macrophages from the mouse peritoneal. The animal was euthanized by cervical dislocation after being reassured and sedated by intraperitoneal injection of a combination of xylazine hydrochloride (10 mg/ kg body weight) and ketamine hydrochloride (80 mg/ kg body weight). The macrophage removal was done in a laminar flow hood with the animal affixed to the dorsal decubitus position by administering 8mL of phosphate buffered saline (PBS – NaCl 145mM, Na_2HPO_4 9mM, Na_2HPO_4 1mM, pH 7,4), sterile at 4°C in the abdominal cavity. Then the abdominal region was softly massaged and aspiration was performed using a needle coupled to a sterile syringe. Based

on the cellular viability morphological the cells were counted in the Neubauer chamber by the Trypan blue exclusion colorimetric method obtaining a minimum of 95% of living cells. Again, the cells were counted using Neutral Red to adjust the desired macrophages concentration (2×10^5 cells/ml).

Peritoneal macrophages were plated per well and incubated on the bacterial cellulosic membrane. After 48h of incubation at 37°C and 5% CO_2 , 10 μL of stained zymosan solution was added and then incubated for 30 min at 37°C . After this procedure, 100 μL of Baker's fixative was added to paralyze the phagocytosis process and after 30 min the plate was washed with 0.9% saline solution to remove zymosan and neutral red that were not phagocytized by macrophages. The supernatant was removed, 100 μL of extraction solution was added and after solubilization on Kline shaker the absorbances were measured at 550 nm in a Biotek plate reader (model ELx800).

Toxicity

For the toxicity analysis the nitric oxide (NO) induction test was performed. Peritoneal macrophages were plated in the amount of 2×10^5 per well and incubated with bacterial cellulosic membrane after 24 hours of incubation at 37°C and 5% CO_2 . Supernatants cells were transferred to another 96 well plate for nitrite dosing. The standard curve was prepared with sodium nitrite in Milli-Q® water at varying concentrations of 1, 5, 10, 25, 50, 75, 100 and 150 μM diluted in the respective culture medium. At the dosing time equal parts of the samples prepared to obtain the standard curve with the same volume of the Griess reagent (1% Sulfanilamide in 10% H_3PO_4 (v: v) in Milli-Q® water, added in parts equal to 0.1% naphthylenediamine in Milli-Q® water) and the absorbances were read on the Biotek plate reader (model ELx800) at 550 nm as a positive control was used Lipopolysaccharide (LPS).

BCM Citotoxicity

The experiments were performed separately on 24-well plates. In the first plate 2×10^5 macrophages were added in 500 μL of supplemented RPMI 1640 medium and 2×10^5 macrophages per well. In the second plate were added 1×10^5 of BMMSC in DMEM supplemented Low Glucose. The plates were incubated at 37°C and 5% CO_2 for 4h for cell adhesion. Two washes were carried out with their respective means for nonadherent cells removal. Subsequently 500 μL

of each medium was added and then the bacterial cellulosic membrane (diameter 15.4mm) was added.

The macrophages plate was incubated for 48 hours and the plate with BMMSC for 7 days, posteriorly added 10% MTT 5 mg/ml diluted in medium. They were incubated for another 4h in a incubator at 37°C with 5% CO₂. The supernatant was discarded and 100 µl of DMSO was added to all wells. The BCM was removed and the plate was shaken for 30 minutes on Kline shaker (model AK 0506) at room temperature for complete dissolution of the formazan. The colorimetric reading was performed in a spectrophotometer at 550 nm in Biotek plate (model ELx800). In the control group the culture media and the respective cultured cells were used under the same conditions.

Statistical analyzes

For the phagocytic capacity analysis, cytotoxicity (MTT) and nitric oxide induction was used the T-Student test for independent samples and the GraphPad Prism version 5.0 software to construct the graphs. These tests were performed in triplicate.

Results

Immediately after the isolation the cells from the BM show to be rounded, dispersed and floating in culture medium. From the first day of culture it was possible to identify undifferentiated cells adherent to the plastic with fibroblastoid morphology. On the fifth day they were still in the adhesion process and on the tenth day they were adhered and arranged in colonies with 80% confluence in a 12-well plate (Fig. 1). After the first peel the cells reached confluence with greater velocity with a five day interval until the confluence of 80% in 25cm² bottles.

The cell cultures after thawing presented viability of 96%, assuming similar characteristics to the primary culture as to its morphology and maintenance of indifferentiation. The observed confluence time was superior to the first repechage of the primary culture. At 3 days the culture showed 80% confluency. In the cell growth curve evaluation were identified two phases (lag, log) corresponding to the cells adaptation period to the culture conditions, the exponential growth period and the stability period with cell growth reduction. Cell concentration data were used to evaluate cell kinetics and are presented in figure 2.

The fibroblastoids colonies proliferation and formation were evident on the 15th day of culture (Fig. 3). The colonies appears of varied sizes, surrounded by empty spaces, distributed throughout the Petri dish area on which macroscopically appear more than 400 colonies. The cells show well-defined cytoplasmic boundaries and nucleus with condensed chromatin regions, and the closer they are to each other, the more elongated cells are arranged parallel to each other (Fig. 4).

Differentiation in BMMSC mesodermal lineages

The cell differentiation assay showed the BMMSC potential to differentiate into chondrogenic and osteogenic strains. The culture induced by chondrogenic differentiation formed a tissue stained in vibrant blue by Alcian Blue and the control presented some spontaneous differentiation fields, cells with fibroblastoid morphology adhered to the culture plate and cytoplasmic integration (Fig. 5).

In the osteogenic induction the culture presented increased deposition of calcium in the extracellular matrix from the 13th day of culture. On the 21st day of induction the culture was very characteristic to osteogenesis. Confirmed after staining with Alizarin Red (Fig. 6A). The negative control showed adhered cells with morphology evidencing spontaneous differentiation foci (Fig. 6B).

BMMSC biointegration to BCM

In the BCM-associated cell culture, BMMSC were adhered to the biomaterial with a fibroblastoid shape and the colonies proliferation and growth were evident at 14 days of culture (Fig. 7).

By means of SEM after 24 hours of cell culture it's possible to observe that the cells rounded shape is still maintained these being subtly anchored to the BCM randomly arranged fibers. In the cultivation carried out for seven days they present themselves in groups forming colonies with several fixation points generating greater adhesion to the biomaterial. Micrographs recorded with 14 days of cell culture show the BMMSC with their cytoplasm fully integrated into the bacterial cellular membrane (Fig. 8).

Macrophage activation and BCM cytotoxicity

In the phagocytic activity assay the T-student test was performed to compare the absorbance resulting from the association of macrophages with cellulose and with the control group (macrophages in the presence of 0.2% DMSO in RPMI 1640 medium). It was observed that in the presence of the bacterial cell membrane the macrophages significantly increased its activity (Fig. 9).

The colorimetric reading of the nitric oxide release showed that the levels remained in a non-cytotoxic concentration for the cells in the presence of BCM (Fig. 10). The difference in NO release between control and BCM was statistically significant at $p < 0.05$ (p-value 0.0184, $t_{0.05}$ -critical: 2.6252) and between LPS and BCM, the difference was considered extremely statistically significant at $p < 0.05$ p-value 0.0001; $t_{0.05}$ -critical: 11.1963).

The tetrazole salt (MTT), incubated with cells in full metabolic activity, showed intense mitochondrial activity (Fig. 11). In this trial, the MTT metabolism by BMMSC showed a statistically significant difference for $p < 0.05$ (p-value 0.0001; $t_{0.05}$ -critical: 2.6252) but there was no statistically significant difference for $p < 0.05$ (p-value 0.0628; $t_{0.05}$ -critical: 2,000) when compared to the control and bacterial cell membrane associated with murine macrophages. In both, cell viability was greater than 94% (Fig. 12).

Discussion

The BMMSC after isolation presented a rounded shape in the culture and in the cell adhesion and expansion process modified their morphology becoming fusiform gradually, proliferating parallel in colonies being perceptible the exclusion of hematopoietic cells in the medium exchanges. Similarly, Samsonraj et al (2015) state that MSCs adhere to favorable surfaces with rapid morphological changes, ranging from rounded to elongated shapes. For Ikebe & Suzuki (2014), adhesion to plastic is the first criterion for the characterization of MSCs. In this cellular adhesion phase, physicochemical connections occur between the cells and the contact surface, including ionic forces that rapidly alter the cell morphology and are evidenced after 1 hour of culture (Pu & Komvopoulos 2014; Wang & He 2016).

The disposition in fibroblast colonies is considered by Kisiel et al (2012), the second characteristic of MSCs. In this experiment the colonies formation was evident after 15 days of the beginning of the primary culture suggesting the occurrence of interactions without cellular

differentiation and therefore a self-renewal with the fibroblastoid morphology maintenance.

Regarding cell viability after thawing, the Lag phase was evident from the first to the fourth day of the growth curve, and the Log phase occurred between the fifth and eleventh day, with exponential mitotic divisions evident mainly between the ninth and eleventh day, and the decline in the number of cell divisions between the twelfth and fifteenth day. Seconda et al. (2015), defines the Lag phase as a relatively short stage characterized by the onset of cell proliferation factors release, the culture remains with the cell population without major modifications. Exponential cell growth (Log phase), second phase, in which the growth rate and duration depends on the medium used, physical conditions (light and temperature), type and cell size. Normally, when cell concentration becomes too high, nutrient depletion, carbon dioxide limitation and light (the shading phenomenon is created between cells) become the main causes of growth decline. When cellular metabolism can no longer be maintained, the cultures undergo apoptosis.

The differentiation ability in more than one mesenchymal lineage (chondrogenic, osteogenic and / or adipogenic) is an important MSCs multipotentiality feature being a fundamental requirement for its characterization (Wuchter, Wagner & Ho 2016). According to Kolf et al. (2015) the tissue formed by chondrogenic cell differentiation, when stained with Alcian Blue, acquires a vibrant blue color and, in the osteogenic differentiation process it's possible to observe the gradual deposition of calcium in the extracellular matrix during the characteristic cell culture attributed to the osteoblasts presence. Evidence of this potential through Alizarin Red staining shows a fairly characteristic reddish coloration. In this study, cell culture using specific media for differentiation into mesodermal (chondrogenic and osteogenic) strains, demonstrated the rabbit BMMSC multipotentiality.

The cell adhesion and proliferation largely depends on the biomaterials surface characteristics, since interactions will occur on these surfaces that will drive the biological responses (Khayyen et al., 2016; CHAHAL, et al., 2016). In this experiment, cell culture showed at 7 days an organization in fibroblastoid format with tendency to cell grouping and in the analysis performed at 14 days, the BMMSC were presented in colonies and close to the total confluence of the BCM surface.

Through SEM it was verified that BM cells maintained their rounded shape on the BCM surface in the first 24 hours with few biomaterial fixation bridges. A delay in the BMMSC

anchoring to BCM was observed when compared to adhesion in culture plates, and this anchoring onset was evidenced in a few hours. For Silveira et al. (2016), the BCM nanofibers three-dimensional structure has an arrangement similar to that of the collagen fibers of the extracellular matrix, and a surface with different pores can provide variable time for cell adhesion to the biomaterial.

The BMMSC anchoring and proliferation to BCM was evident on the seventh day of culture with grouped cells and several cytoplasmic projections points in BCM. On the 14th day of culture an excellent BMMSC fixation with strong interaction with the biomaterial is evidenced. Thus corroborating with Alberti & Xu, (2016) and Santana, et al. (2014), the presence of cytoplasmic projections and normal cell morphology are factors that confirm the cytocompatibility between BCM scaffold and cells.

The equilibrium in the immune system cells activation also reflect the tissue regenerative quality. Thus in the presence of the cellulosic membrane, the macrophages presented a statistically significant increase for $p < 0.05$ (p-value 0.0002; $t_{0.05}$ -critical: 4.8118) in their activity when compared to the control group. For QIU, et al. (2016) clarifies that maintaining scaffold intact in the period of adhesion and cell proliferation is important for the regenerative process quality and architecture of the tissue to be repaired. Gradually the implantable biomaterial should biodegrade to give rise to the newly formed tissue without exacerbating an inflammatory response that compromises the repair quality thus the adequate inflammatory response of the host in specific situations makes the biomaterial compatible with its use.

The bacterial cellulose (BC) degradability has not yet been fully elucidated. In animal and human tissues it's considered limited due to the absence of hydrolases that rupture the β (1,4) binding of the cellulose chain that is responsible for the solubility of the biomaterial (Oliveira, Rambo & Porto, 2013). Although the idea of a completely degradable scaffold is interesting from the point of view of tissue engineering there are still difficulties faced with materials with this property since the degradation time synchronization and tissue repair combined with the mechanical properties acquired by the newly formed tissue lead researchers to believe that a material with a low rate of degradation may respond better when the cicatricial process requires more time-consuming conditions (Bhattacharjee, et al., 2015).

After inflammation, macrophages release nitric oxide (NO) as a way to eliminate pathogens. In addition, NO is known as a inflammatory response mediator inhibiting or inducing

inflammation according to the concentration of NO released (Taraballi, et al., 2016). The colorimetric nitrite dosage produced by macrophages treated in the presence of the bacterial cellulosic membrane showed a non-cytotoxic concentration for the cells, approaching the value obtained in the control group.

The MTT test is a detection method and cell viability widely used to evaluate the MTT metabolism by the mitochondria of viable cells when being incubated with cells in full metabolic activity crosses the plasma membrane and, when coming in contact with the superoxide produced by the mitochondrial activity is reduced by succinate dehydrogenase present in MTT-formazan mitochondria. The crystals formed are insoluble in water, however they are solubilized in DMSO medium and show violet coloration. Thus, cell viability is directly proportional to the intensity of staining (Toh, Yap & Lim, 2015). For Li, Zhou & Xu (2015), a material is considered non-cytotoxic and biocompatible when values for cell viability are greater than 70%. In this study, the MTT assay presented intense violet placement of the crystals, evidencing that BCM does not provide a toxic effect on the cells and, 94% cellular viability is considerably favorable for non-interference of cellular activity.

Conclusion

The expansion and cellular integration to the biomaterials greatly depends on the quality and suitability of the biomaterial surface. The bacterial cellulosic membrane allowed the adhesion, expansion and bone marrow stem cells biointegration maintaining the BCM cytotoxicity and toxicity considerably viable for cell culture. Macrophage activation and the BCM degradation velocity makes it an ideal biomaterial for slow healing processes in which reconstructed tissues require a *scaffold* with longer durability.

Considering the demonstrated interaction between BMMSC and BCM it can be stated that BCM is a promising biomaterial in tissue engineering and regenerative medicine. However it's necessary to test the *in vivo* BCM implants behavior in diversified time periods.

Acknowledgments

We thank the National Council for Scientific and Technological Development – CNPq (Process: 427626 /2016-1) for financial support.

The Integrated Nucleus of Morphology and Stem Cell Research (NUPCelt), Interdisciplinary Laboratory of Advanced Materials (LIMAV), Advanced Microscopy Multiuser Laboratory (LMMA) and Antileishmania Activity Laboratoy (LAA) from the Federal University

of Piauí – UFPI as well as the Laboratory of Toxicological Research – LAPETOX of University of Sorocaba – UNISO.

The protocol was approved by the Committee on Ethics in the animals use of the Federal University of Piauí (CEUA-UFPI, Permit Number 268/16).

ADDITIONAL INFORMATION AND DECLARATIONS

Funding

This work had the financial support of the National Council of Scientific and Technological Development – CNPq (Process: 427626/2016-1).

Grant Disclosures

The following grant informations was disclosed by the authors:

CNPq (Process: 427626/2016-1)

Integrated Nucleus of Morphology and Stem Cell Research – NUPCelt.

National Council of Scientific and Technological Development – CNPq (Process: 427626/2016-1)

Competing Interests

The authors declare there are no competing interests.

Authors contributions

- Marcello Silva performed the experiments, analyzed the data, wrote the document, prepared the figures and revised the manuscript drafts.
- Yulla Leite, Camila Carvalho, Matheus Feitosa contributed with tools and figures analysis.
- Angela Jozala prepared and yielded the bacterial cellulosic membrane.
- Acelina Martins de Carvalho, Maria Angelica Miglino conceived and designed the experiments, revised manuscript.

Ethics Committee

The study was carried out in accordance with the recommendations of the Guide for the Laboratory Animals Care and Use of the National Institute of Health. The protocol was approved by the Ethics Committee on Animal Use of the Federal University of Piauí (CEUA-UFPI, permit number: 268/16).

References

- Abbott R, Kaplan D. 2016.** Engineering Biomaterials for Enhanced Tissue Regeneration, *Current Stem Cell Reports*, **22(2)**:140-146. DOI: 10.1007/s40778-016-0039-3.
- Achatz F, Kujat R, Pfeifer C, Koch M, Nerlich M, Angele P, Zellner J. 2016.** *In Vitro* Testing of *Scaffolds* for Mesenchymal Stem Cell-Based Meniscus Tissue Engineering—Introducing a New Biocompatibility Scoring System, *Materials*, **9(4)**:1-14 DOI: 10.3390/ma9040276.
- Agatha H. Kisiel DVM, Laurie A, Mcduffee DVM, Masaoud E, Bailey TR, Gonzalez BPE, Fong-Nino R. 2012.** Isolation, characterization, and *in vitro* proliferation of canine mesenchymal stem cells derived from bone marrow, adipose tissue, muscle, and periosteum, *American Journal of Veterinary*, **73(8)**:1305-1317 DOI 10.2460/ajvr.73.8.1305.
- Alberti KA, Xu Q. 2016.** Biocompatibility and degradation of tendon-derived *scaffolds*, *Regenerative biomaterials*, **1(1)**:1-11 DOI 10.1093/rb/rbv023.
- Bhattacharjee M, Coburn J, Centolo M, Murab S, Barbero A, Kaplan DL, Martin I, Ghosh S. 2015.** Tissue engineering strategies to study cartilage development degeneration and regeneration. *Advanced Drug Delivery Reviews*. **85**:107-122.
- Blanquer SBG, Grijpma DW, Poot AA. 2015.** Delivery systems for the treatment of degenerative intervertebral discs. *Advanced Drug Reviews*. **84**:172-187 DOI 10.1016/j.addr.2014.10.024.
- Castellanos AM, Balkan W, DiFede DL, Hare JM. 2016.** Cell infection site influences the human mesenchymal stem cell therapy effectiveness for left ventricular dysfunction in ischemic cardiomyopathy. *Circulation*. **123(1)**:A192102 DOI 10.1161/CIRCULATIONAHA.116.024610.
- Chahal S, Hussain FSJ, Kumar A, Rasad MSBA, Yusoff MM. 2016.** Fabrication, characterization and *in vitro* biocompatibility of electrospun hydroxyethyl cellulose/poly (vinyl) alcohol nanofibrous composite biomaterial for bone tissue engineering, *Chemical Engineering Science*, **144(22)**:17-29 DOI 10.1016/j.ces.2015.12.030.
- Cruz IBM, SEVERO AL, Azzolin VF, Garcia LFM, Kuhn A, Lech O. 2016.** Potencial regenerativo do tecido cartilaginoso por células-tronco mesenquimais: atualização, limitações e desafios. *Revista Brasileira de Ortopedia*. 1-9 DOI 10.1016/j.rbo.2016.02.007.

- 497 **DiMarino AM, Caplan AI & Bonfield TL. 2013.** Mesenchymal stem cells in tissue repair.
498 *Frontier in Immunology*, 4:1-9 DOI 10.3389/fimmu.2013.00201.
- 499
- 500 **Emmet TM, Amos M, Daniel KJ, John GP, O'Brien FJ. 2016.** An Endochondral
501 Ossification-Based Approach to Bone Repair: Chondrogenically Primed Mesenchymal Stem
502 Cell-Laden Scaffolds Support Greater Repair of Critical-Sized Cranial Defects Than
503 Osteogenically Stimulated Constructs In Vivo. *Tissue Engineering Part A*. **22(5-6)**: 556-567 DOI
504 10.1089/ten.tea.2015.0457.
- 505
- 506 **Fávaro RC, Arruda AO, Vialle LR, Vialle EN. 2016.** Influência da terapia celular
507 mononuclear sobre a degeneração discal em coelhos. *Revista Brasileira de Ortopedia*. **1(9)**. DOI
508 10.1016/j.rbo.2016.03.007.
- 509
- 510 **Fu L, Zhang J, Yang G. 2013.** Present status and applications of bacterial cellulose-based
511 materials for skin tissue repair. *Carbohydrate Polymers*. **92**:1431-1442.
- 512
- 513 **Ikebe C, Suzuki K. 2014.** Mesenchymal Stem Cells for Regenerative Therapy: optimization of
514 Cell Preparation Protocols, *Biomed Research International*. **1(1)**:1-11 DOI
515 10.1155/2014/951512.
- 516
- 517 **Kaplan JM, Youd ME, Lodie TA. 2011.** Immunomodulatory activity of mesenchymal stem
518 cells. *Current Stem Cell Research & Therapy*. **6(4)**:297-316 DOI
519 10.2174/157488811797904353.
- 520
- 521 **Khayyeri H, Longo G, Gustafsson A, Isaksson H. 2016.** Comparison of structural anisotropic
522 soft tissue models for simulating Achilles tendon tensile behavior. *Journal of the mechanical*
523 *behavior of biomedical materials*, **6(1)**:431-443 DOI /10.1016/j.jmbbm.2016.04.007.
- 524 **Kim M, Kim G. 2015.** 3D multi-layered fibrous cellulose structure using an
525 electrohydrodynamic process for tissue engineering. *Journal of Colloid and Interface Science*.
526 **457**:180-187. DOI 10.1016/j.jcis.2015.07.007.
- 527
- 528 **Kolf CM, Song L, Helm J, Tuan RS. 2015.** “Nascent osteoblast matrix inhibits osteogenesis of
529 human mesenchymal stem cells *in vitro*”. *Stem Cell research & Therapy*, **22(6)**:1-16 DOI
530 10.1186/s13287-015-0223-x.
- 531
- 532 **Langer R, Vacanti J. 2016.** Advanced in tissue engineering, *Journal of Pediatric Surgery*,
533 **1(51)**:8-12 DOI 10.1016/j.jpedsurg. 2015.10.022.
- 534
- 535 **LI W, Zhou J, Xu Y. 2015.** Study of the in vitro cytotoxicity testing of medical devices
536 (Review). *Biomedical Reports*. **3**: 617-620 DOI 10.3892/br.2015.481.

- 537
- 538 **Li X, Yuan Z, Wei X, LI H, Zhao G, Miao J, Wu D, Liu B, Cao S, An D, Ma W, Zhang H,**
- 539 **Wang W, Wang Q, Gu H. 2016.** Application potencial of bone marrow mesenchymal stem cell
- 540 (BMSCs) based tissue-engineering for spinal cord defect repair in rat fetuses with spina bifida
- 541 aperta, *Tissue engineering constructs and cell substrates*, **27(4)**: 1-11 DOI 10.1007/s10856-016-
- 542 5684-7.
- 543
- 544 **Lin WC, Lien CC, Yeh HJ, Yu CM, Hsu SH. 2013.** Bacterial cellulose and bacterial cellulose-
- 545 chitosan membranes for wound dressing applications. *Carbohydrate Polymers*. **94**: 603-611 DOI
- 546 10.1016/j.carbpol.2013.01.076.
- 547
- 548 **Oliveira VA, Rambo CR, Porto LM. 2013.** Produção e degradação in vitro de estruturas
- 549 tubulares de celulose bacteriana. *Polimeros*. DOI 10.4322/polimeros.2013.041.
- 550
- 551 **Peach MS, Ramos DM, James R, Morozowich NL, Mazzocca AD, Doty SB, Allcock HR,**
- 552 **Kumbar SG, Laurencin CT. 2017.** Engineered stem cell niche matrices for rotator cuff tendo
- 553 regenerative engineering. *Plos One*. 1-19. DOI 10.1371/journal.pone.0174789.
- 554
- 555 **Pires A, Bierhalz A, Moraes A. 2015.** Biomateriais: tipos, aplicações e mercado, *Química nova*,
- 556 **38(7)**: 957-971 DOI 10.5935/0100-4042.20150094.
- 557
- 558 **PU J, Komvopoulos K. 2014.** Mechanical properties of electrospun bilayer fibrous membranes
- 559 as potential *scaffolds* for tissue engineering, *Acta Biomaterialia*, **10(1)**:2718-2726. DOI
- 560 10.1016/j.actbio.2013.12.060.
- 561
- 562 **Qiu Y, Qiu L, Cui J, Wei Q. 2016.** Bacterial cellulose and bacterial cellulose-vaccarin
- 563 membranes for wound healing. *Materials Science and Engineering C*. **59**:303-309.
- 564
- 565 **Rajwade JM, Paknikar KM, Kumbhar JV. 2015.** Applications of bacterial cellulose and its
- 566 composites in biomedicine. *Appl Microbiol Biotechnol*. **99**:2491-2511. DOI 10.1007/s00253-
- 567 015-6426-3.
- 568
- 569 **Samsonraj RM, Rai B, Sathiyathan P, Puan KJ, Röttschke O, Hui JH, Raghunath M,**
- 570 **Stanton LW, Nurcombe V, Cool SM. 2015.** Establishing Criteria for Human Mesenchymal
- 571 Stem Cell Potency, *Translational and Clinical Research*, **1(1)**:1878-1891 DOI
- 572 10.1002/stem.1982.
- 573
- 574 **Santana CC, Nóbrega Neto PI, Sá MJC. 2014.** Utilização do filme de quitosana na reparação
- 575 de tendão em coelhos. *Arquivo brasileiro de medicina veterinária e zootecnia*, **66(4)**:995-1002
- 576 DOI 10.1590/1678-6521.

- Schnitzler AC, Verma A, Kehoe DE, Jing D, Murrell JR, Der KA, Aysola M, Rapiejko PJ, Punreddy S, Rook MS. 2016.** Bioprocessing of human mesenchymal stem/stromal cells for therapeutic use: Current technologies and challenges. *Biochemical Engineering Journal*. **108**:3-13.
- Secunda R, Vennila R, Mohanashankar AM, Rajasundari S, Surendran R. 2015.** Isolation, expansion and characterisation of mesenchymal stem cells from human bone marrow, adipose tissue, umbilical cord blood and matrix: a comparative study, *Cytotechnology*, **67(5)**:793-807 DOI: 10.1007/s10616-014-9718-z.
- Silveira RK, Coelho ARB, Pinto FCM, Albuquerque AV, Filho DAM, Aguiar, JLA. 2016.** Bioprosthetic mesh of bacterial cellulose. *Materials in Medicine*, **27(8)**:1-9 DOI: 10.1007/s10856-016-5744-z.
- Soheilmoghaddam M, Sharifzadeh G, Pour RH, Wahit MU, Whye WT, Lee XY. 2014.** Regenerated cellulose/ β -cyclodextrin scaffold prepared using ionic liquid. *Material Letters*. **135**: 210-2013 DOI: 10.1016/j.matlet.2014.07.169.
- Squillaro T, Peluso G, Galderisi. 2016.** Clinical trials with mesenchymal stem cells: an update. *Cell Transplantation*, **25**:829-848 DOI:10.3727/096368915X689622.
- Taraballi F, Corradetti B, Minardi S, Powel S, Cabrera F, Van Eps JL, Weiner BK, Tasciotti E. 2016.** Biomimetic collagenous scaffold to tune inflammation by targeting macrophages. *Journal of Tissue Engineering*. **7**:1-13 DOI: 10.1177/204173141524667.
- Toh WS, Yap AUJ, Lim SY. 2015.** In vitro biocompatibility of contemporary bulk-fill composites. *Operative Dentistry*. **40(6)**:644-652. DOI 10.2341/15-059-L.
- Urbina L, Algar I, García-Astrain C, Gabilondo N, González A, Corcuera MA, Eceiza A, Retegi A. 2016.** *Journal of Applied Polymer*. 1-10 DOI: 10.1002/APP.43669.
- Wang S, Qu X, Zhao R.C. 2012.** Clinical applications of mesenchymal stem cells. *Journal of Hematology & Oncology*, **19(5)**:1-9.
- Wang W, He J, Feng B, Zhang Z, Zhou G, Cao Y, Fu W, Liu W. 2016.** Aligned nanofibers direct human dermal fibroblasts to tenogenic phenotype *in vitro* and enhance tendon regeneration *in vivo*, *Nanomedicine*, **11(9)**:1055-1072 DOI: 10.2217/nnm.16.24.
- Wei X, Yang X, Han Z, Qu F, Shao L, Shi Y. 2013.** Mesenchymal stem cells: a new trend for cell therapy, *Acta Pharmacologica Sinica*, **34(6)**:747-754 DOI: 10.1038/aps.2013.50.

Wuchter P, wagner W, Ho A.D. 2016. Mesenchymal Stromal Cells (MSC). IN: Regenerative Medicine – From protocol to Paciente. 3 ed. Switzerland: Springer.

Xi J, Yan X, Zhou J, Yue W, Pei X. 2013. Mesenchymal stem cells in tissue repairing and regeneration: Progress and future. *Burns & Trauma*, **1(1)**:13-20.

Zhao Q, Ren H, Han Z. 2016. Mesenchymal stem cells: Immunomodulatory capability and clinical potencial in imune diseases. *Journal of Cellular Immunotherapy*, **2**:3-20 DOI: 10.1016/j.jocit.2014.12.001.

Zulkifli FH, Hussain FSJ, Rasad MSA, Yusoff MM. 2014. Nanostructure materials from hydroxyethyl cellulose for skin tissue engineering. *Carbohydrate Polymers*. **144**:238-245 DOI: 10.1016/j.carbpol.2014.08.019.

Figure 1

BMMSC culture and expansion photomicrography

(A) rabbit cells newly isolated from bone marrow in a 12-well plate (objective 4x, bar: 50µm)
 (B) cells in the adhesion process on the fifth day of cell culture performed on a plate 12 wells (objective 20x, bar: 25µm), (C) cells arranged parallel in fibroblastoid format with confluence of 80% in the tenth day of cell culture in 12-well plate (objective 10x, bar: 50µm), (D) and (E) cytoplasmic adhesion and expansion process with 80% confluence in 25cm² bottle after trypsinization and 15th day of cell culture (objective 10x, bar: 50µm), (F) cells with fibroblastoid morphology arranged in parallel and in colonies with 80% of confluence in 25cm² bottle after trypsinization and 20th day of cell culture (10x objective, bar: 50µm).

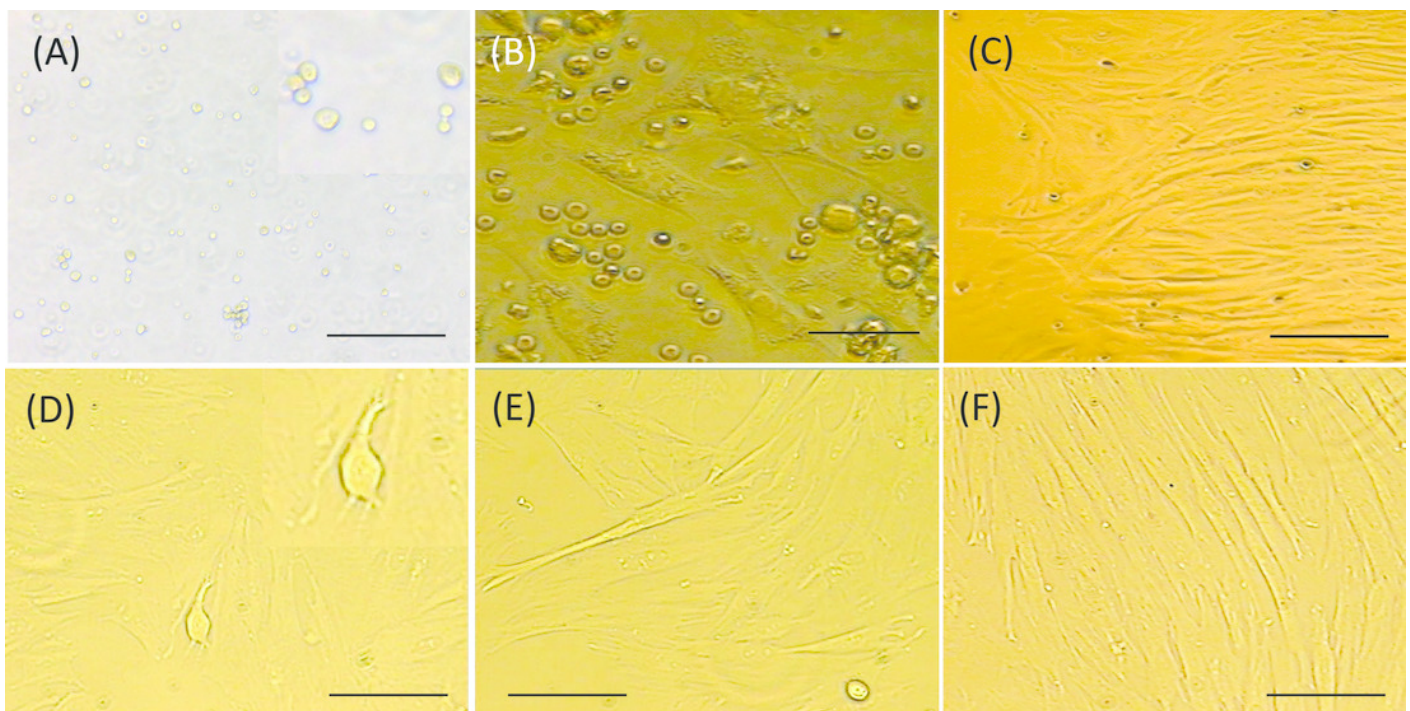


Figure 2

Growth curve

Stem cells duplicate derived from rabbit bone marrow during 15 days after thawing cultured at 1×10^4 cel/ml concentration. The phases in evidence: LAG (1st to 4th day), LOG (5th to 11th day) and culture decline (12th to 15th day).

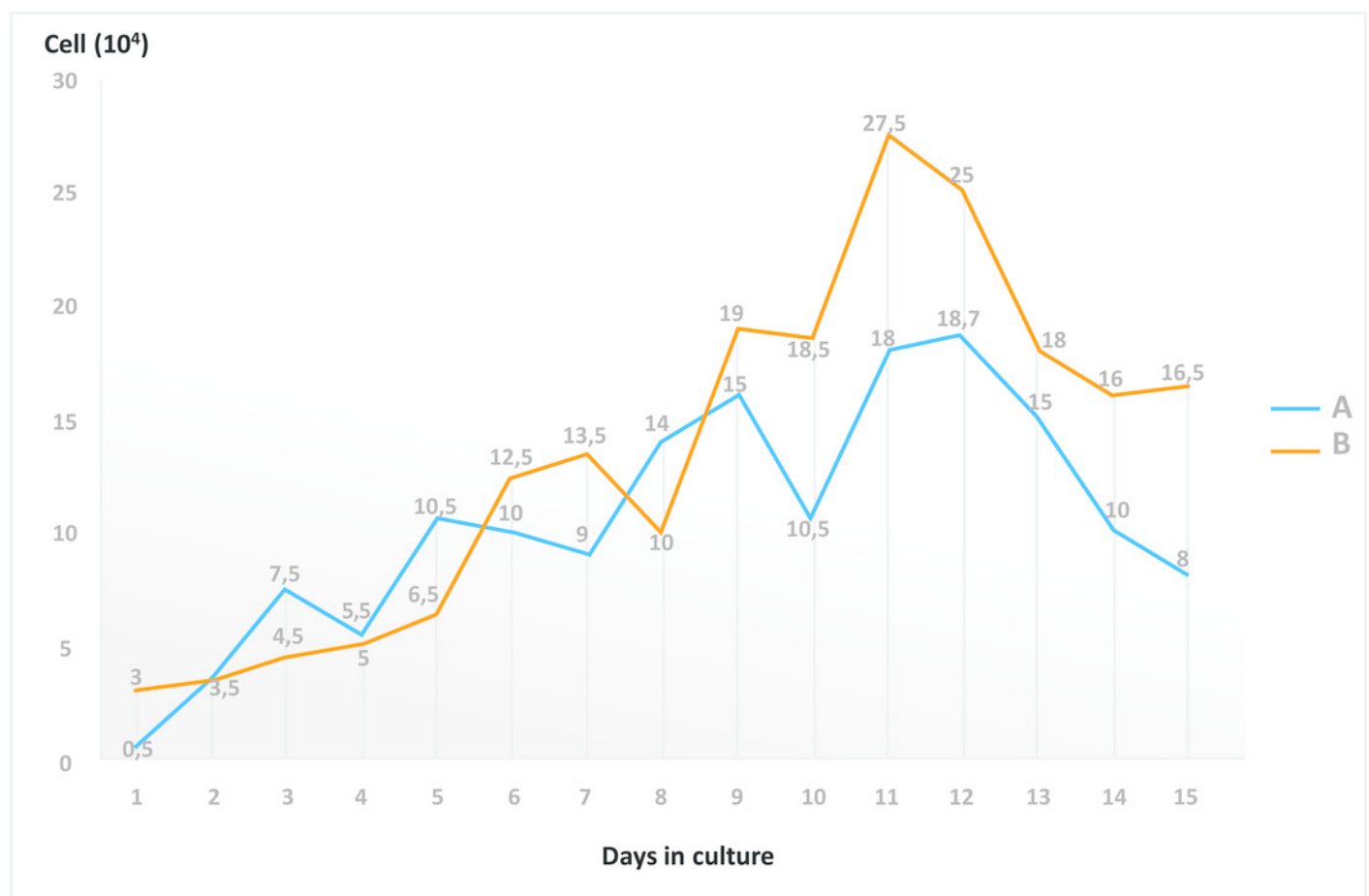


Figure 3

Fibroblastoid colony forming cell assay

Photomicrography of Giemsa-stained BMMSC colonies in Petri dishes 90x15mm after 15 days of cell culture 80% confluence (objective 4x, bar: 50µm).

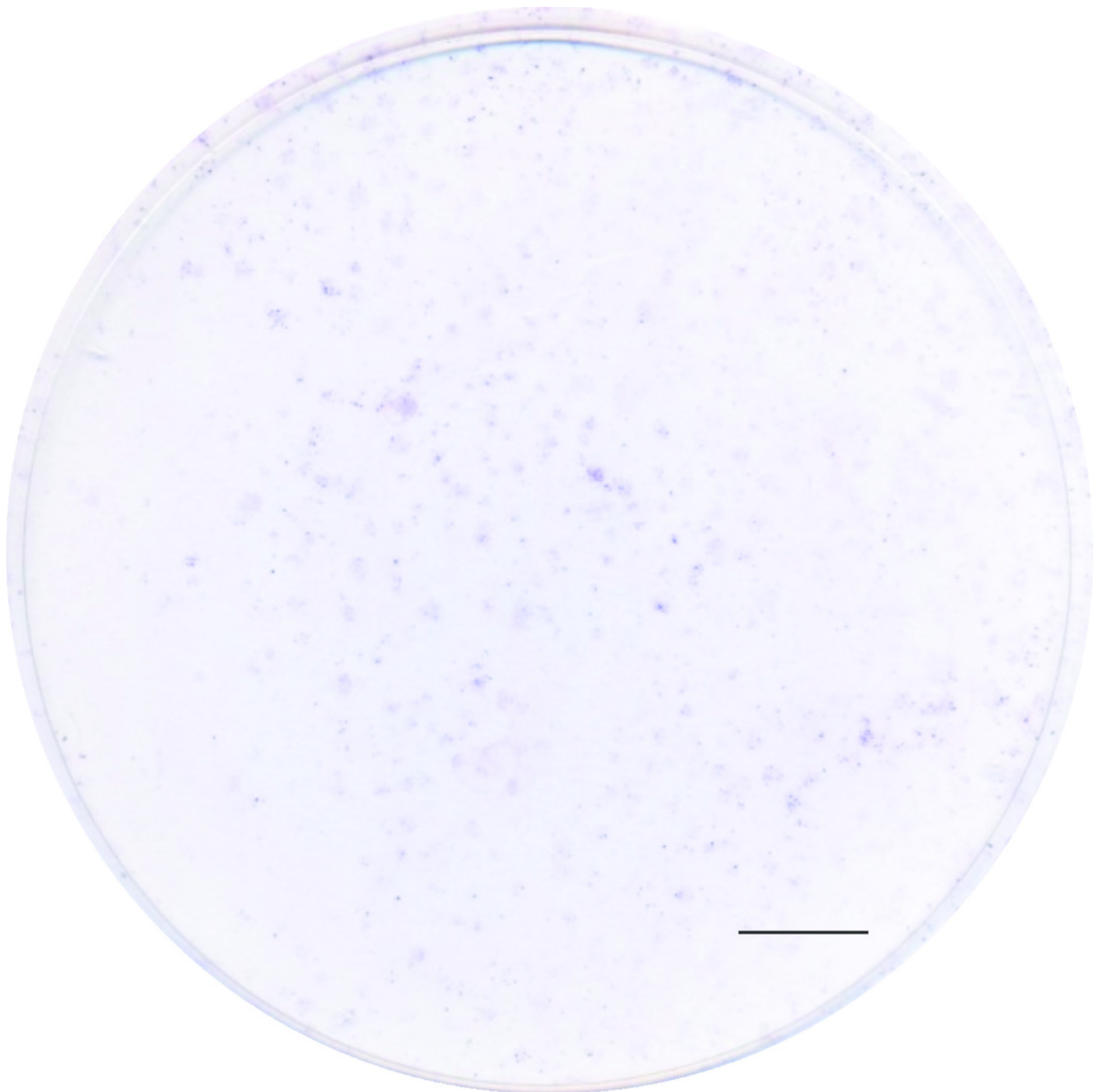


Figure 4

BMMSC colonies photomicrography

(A) colonies with more than 30 cells per field (objective 10x, bar: 50 μ m), (B) colonies with more than 30 cells per field in Petri dishes 90x15mm (objective 20x, bar: 25 μ m).

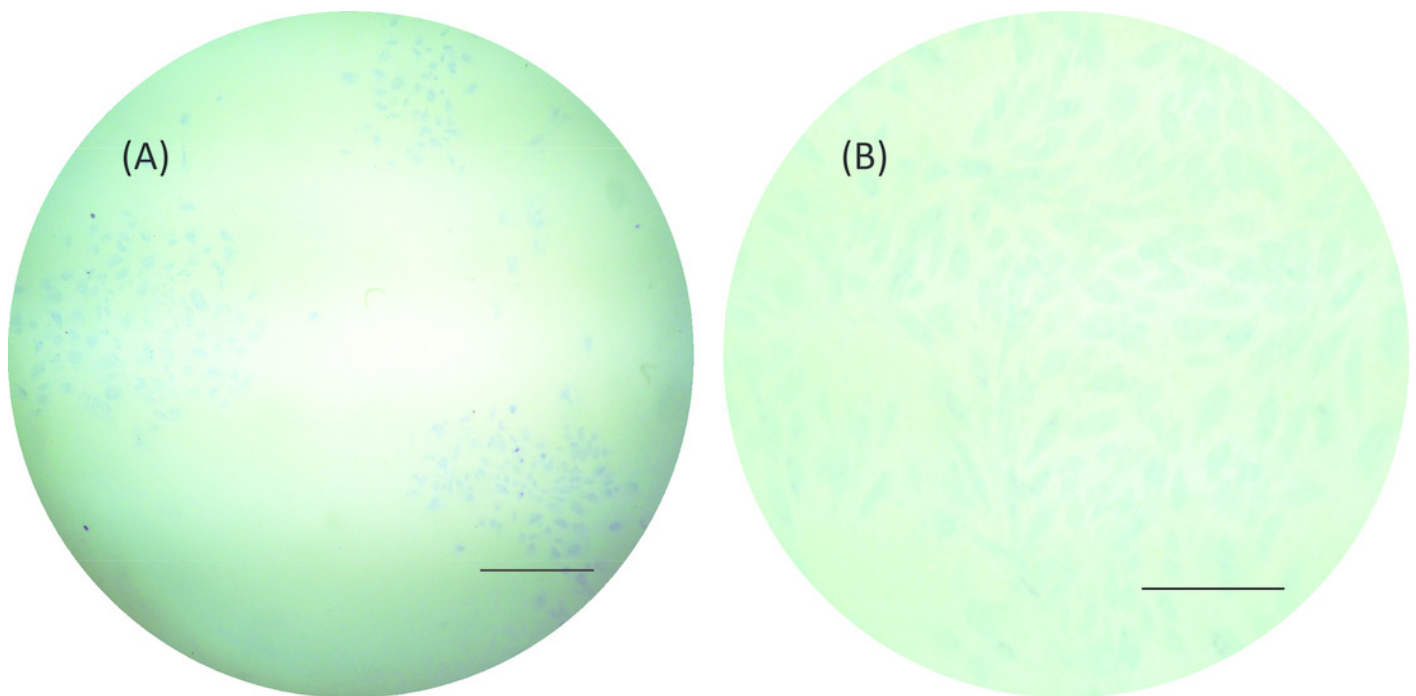


Figure 5

Photomicrographs showing BMMSC differentiation

(A) BMMSC chondrogenic differentiation (objective 20x, bar: 25 μ m), (B) negative control for 14 day differentiation of chondrogenic (objective 10x bar: 25 μ m).

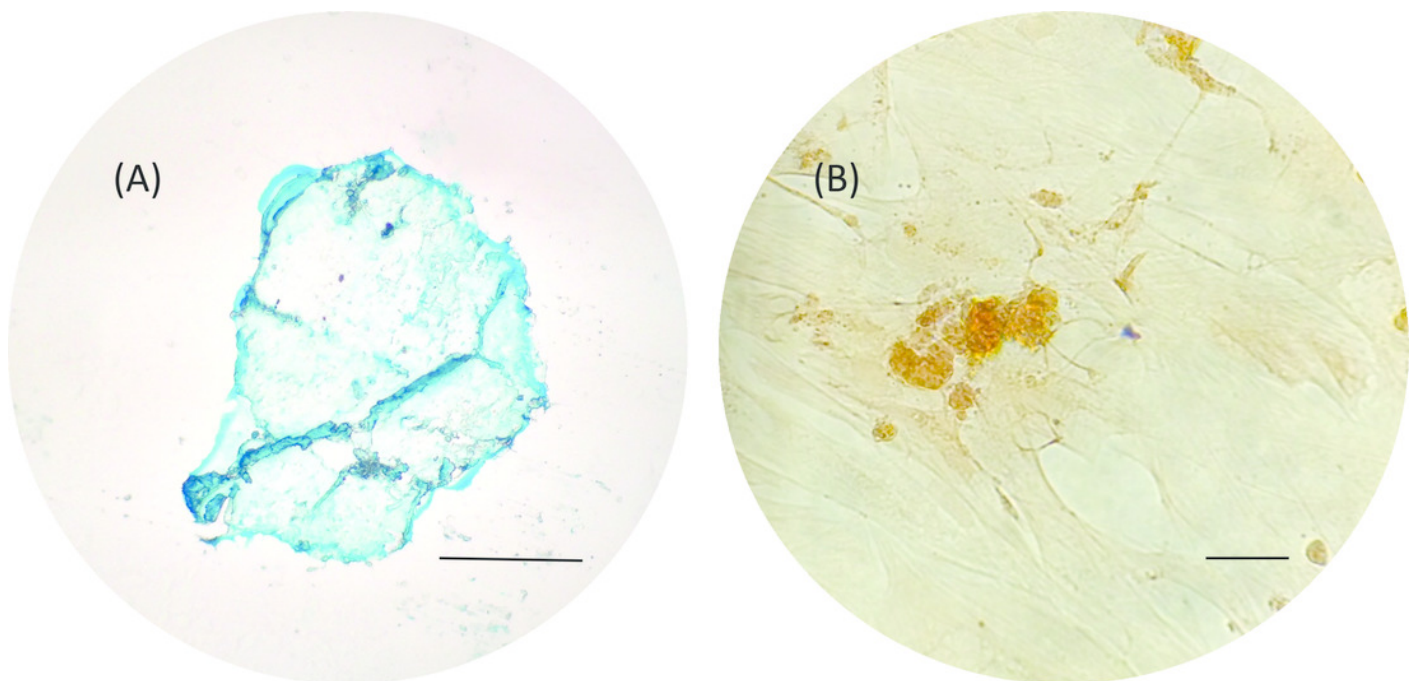


Figure 6

Photomicrographs showing BMMSC differentiation

(A) BMMSC osteogenic differentiation showing calcium rich deposition in the extracellular matrix (objective 10x, bar: 25 μ m), (B) negative control for osteogenic differentiation for 21 days (objective 10x, bar: 25 μ m).

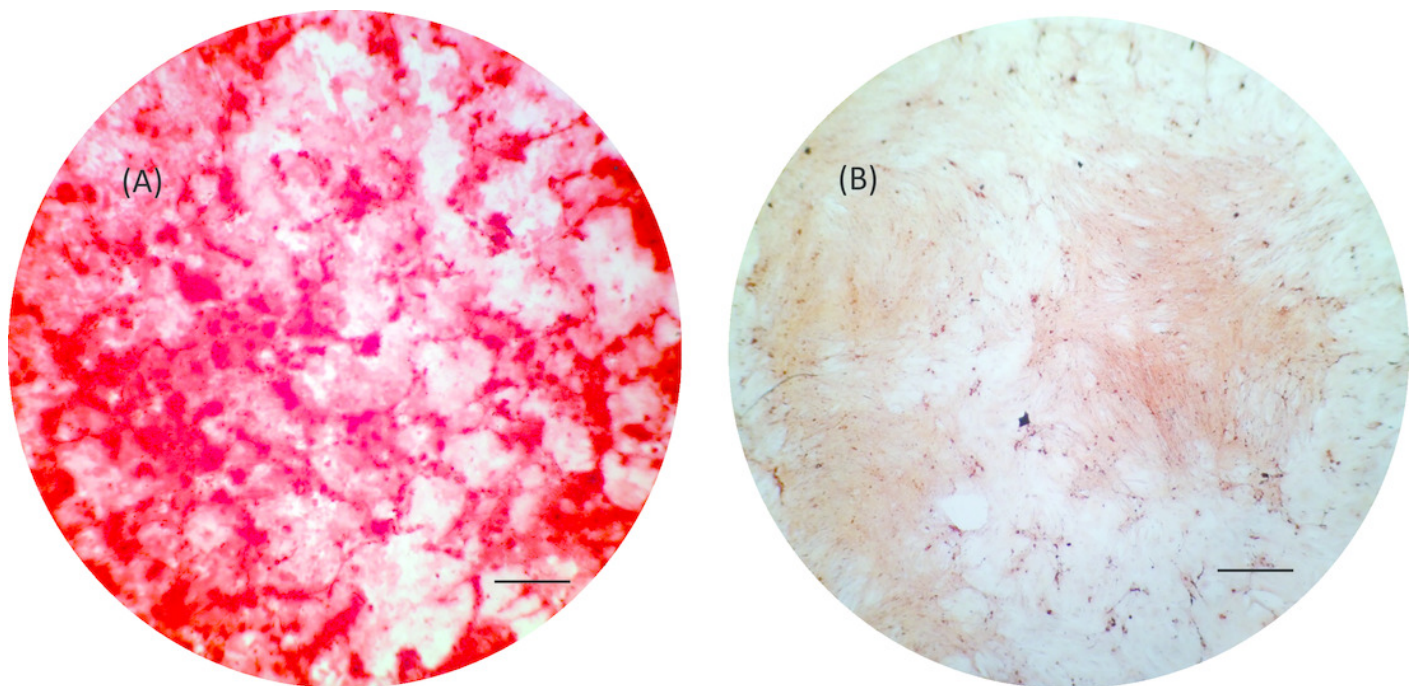


Figure 7

BMMSC photomicrography adhered to the bacterial cellulosic membrane

(A) BMMSC adhesion after seven days of cell culture, highlighting the formation of CFC-F on BCM (objective 20x, bar: 25 μ m), (B) BMMSC colonies with 14 days of cell culture (objective 10x, bar: 50 μ m).

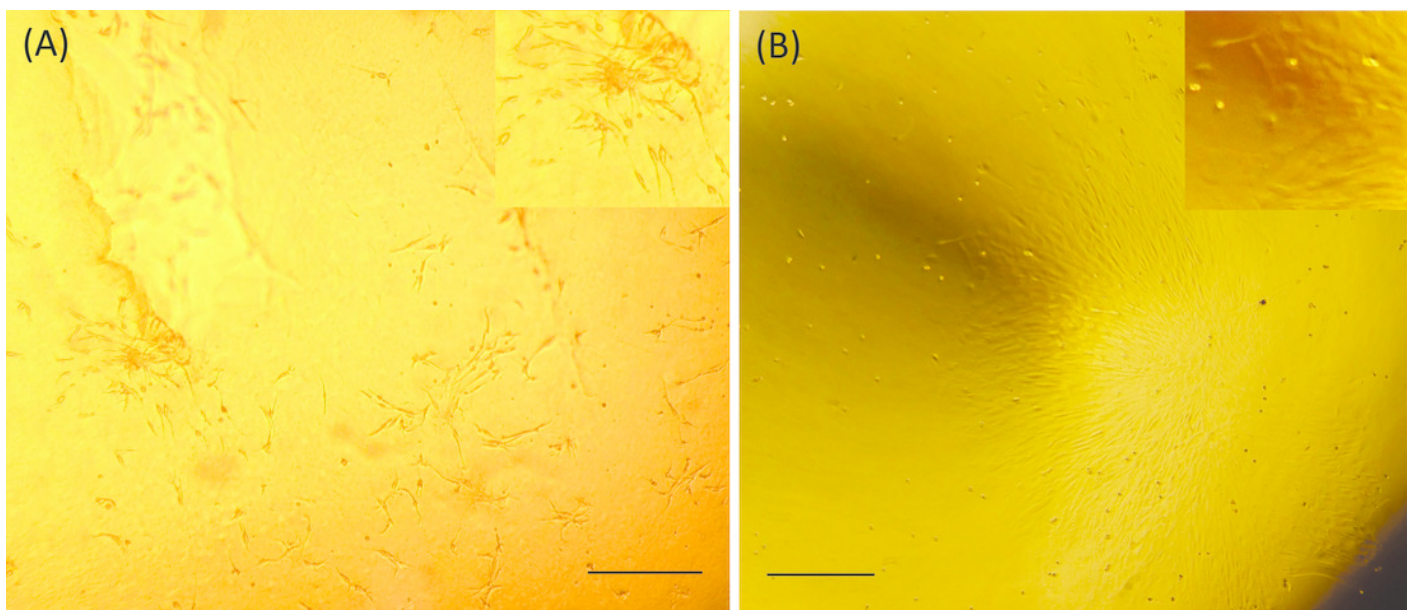


Figure 8

Scanning Electron Microscopy (SEM) showing BMMSC anchorage and biointegration to the bacterial cellulose membrane

(A) and (B) analysis after 24 hours of cell culture, increase of 10,000x and 20,000x respectively, (C) and (D) with seven (E) and (F) after 14 days of cell culture, 40,000x and 16,000x respectively.

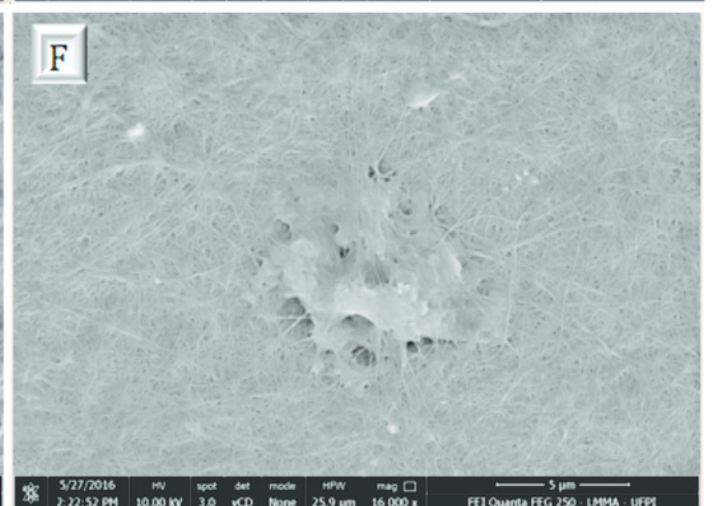
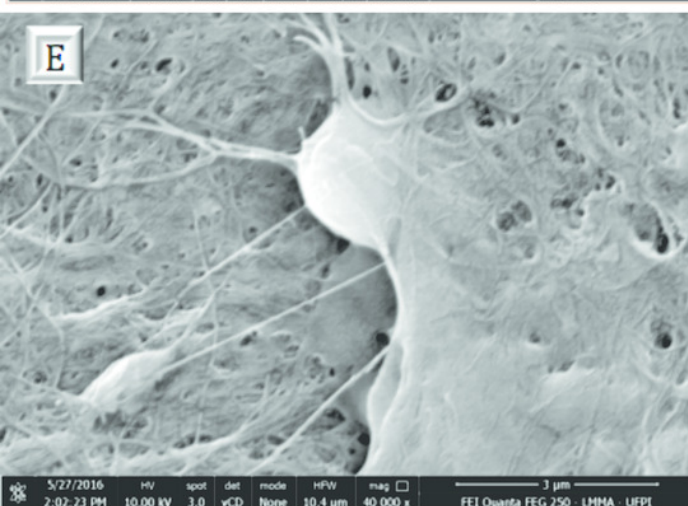
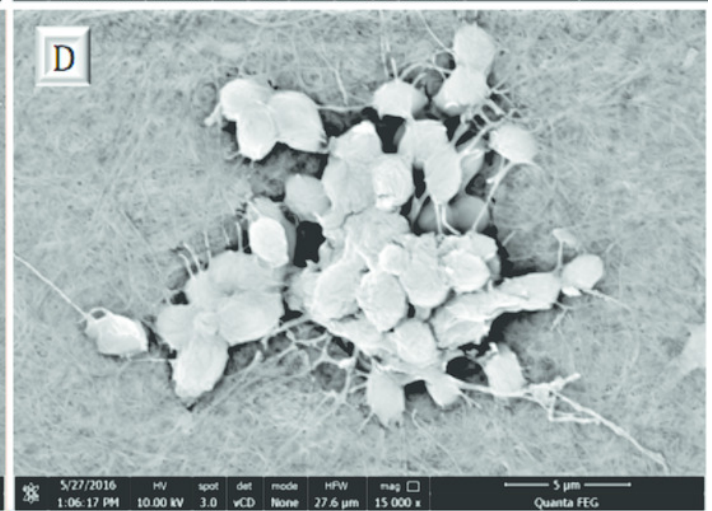
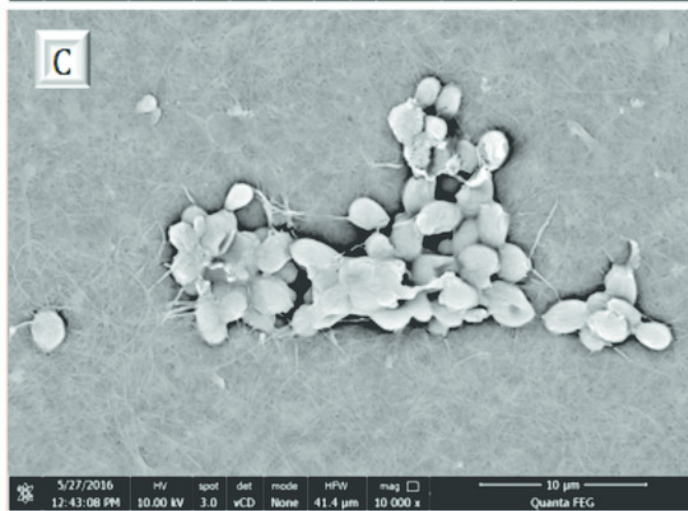
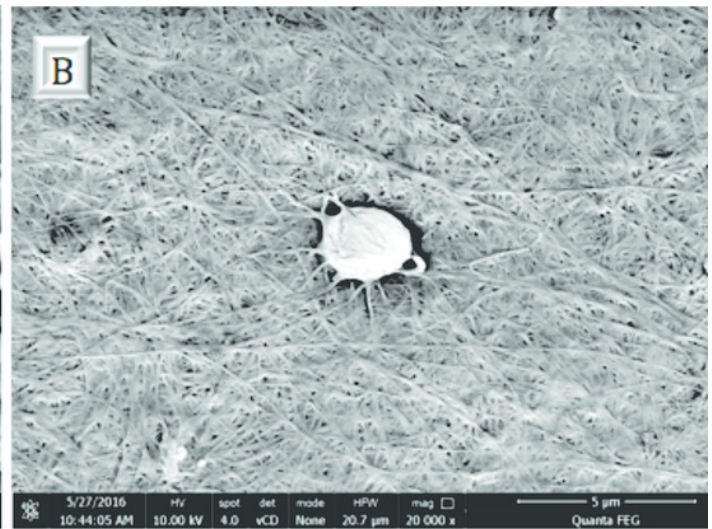
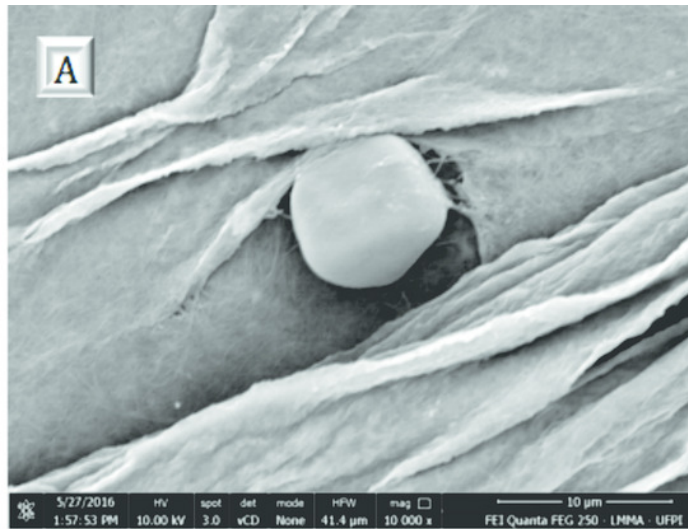


Figure 9

Zymosan particles phagocytosis by macrophages in the presence of bacterial cellulosic membrane

The graph represents the mean \pm standard error of the mean of three independent experiments performed in triplicate (control: mean 0.28567, standard deviation 0.03161; BCM: mean 0.36100, standard deviation 0.03474). ABS - Absorbance, C - Control and MCB - Cellulosic bacterial membrane, * $p < 0.05$.

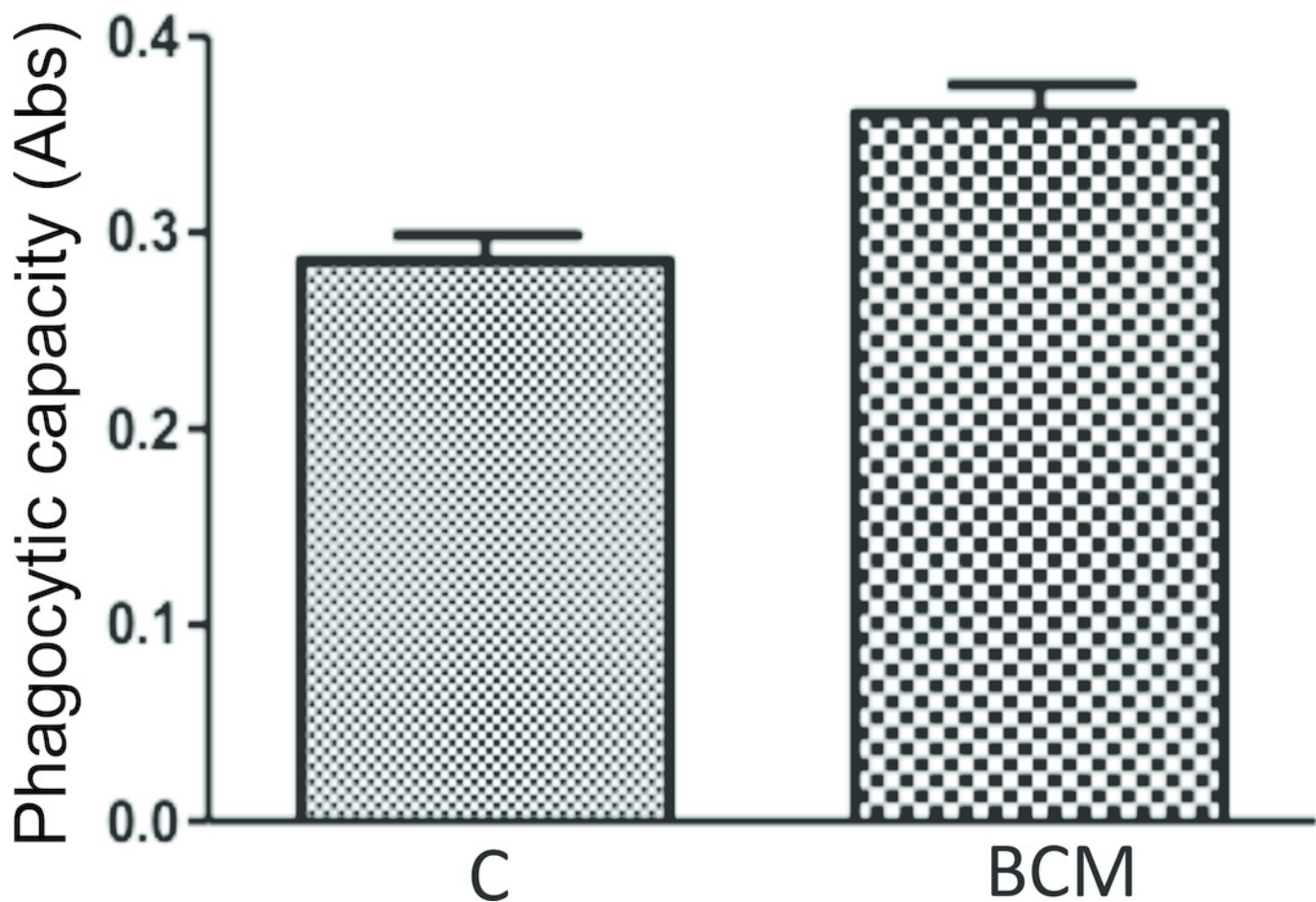


Figure 10

Colorimetric nitrite dosage produced by macrophages, treated with LPS and in the presence of bacterial cellulosic membrane

The plot represents the mean \pm standard error of the average of three independent experiments performed in triplicate (control: mean 100.0000, standard deviation 0.0000, LPS: mean 150.8889, standard deviation 1.0541, BCM: mean 109.6300, standard deviation 11.0047). T-Student test was performed for comparison between groups with the control (0.2% DMSO in RPMI 1640 medium), being * $p < 0.05$. C - Control, LPS - Lipopolysaccharide and BCM - Bacterial cellulosic membrane.

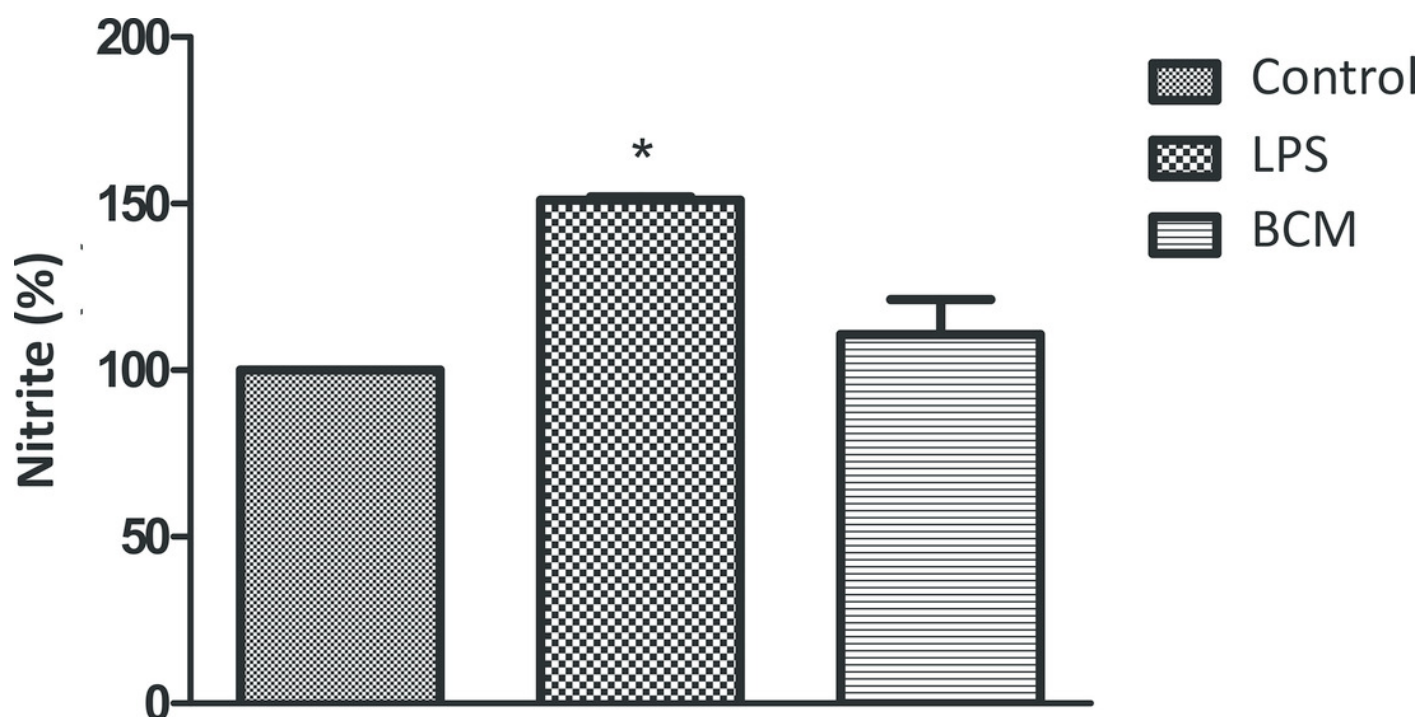


Figure 11

Formazan crystals in bacterial cellulosic membrane cultured with

A) Bone marrow mesenchymal stem cells B) Peritoneal macrophages. Increasing view 40x.

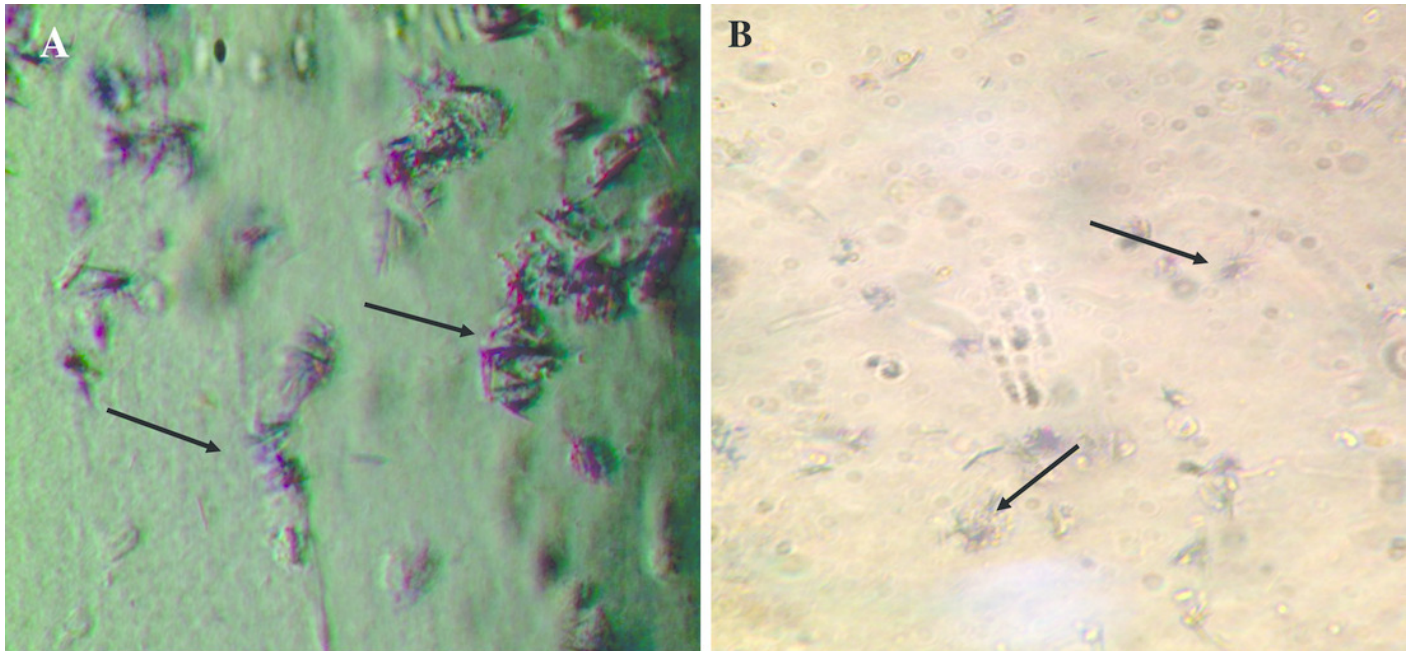


Figure 12

Bacterial cellulosic membrane effect on the BMMSC viability and mammalian peritoneal macrophages

A) BMMSC viability in BCM (control: mean 100.0000, standard deviation 0.0000, BCM: mean 94.4533, standard deviation 1.1926); B) murine macrophages viability in bacterial cellulosic membrane (control: mean 100.0000, standard deviation 0.0000, BCM: mean 97.7867, standard deviation 3.3200). The plot represents the mean \pm standard error of the average of three independent experiments performed in triplicate. T-student test was performed to compare the groups with the control (0.2% DMSO in DMEM / RPMI medium) being * $p < 0.05$. C - Control and BCM - Bacterial cellulosic membrane.

